Sustainable Development and Innovations in Marine Technologies – Georgiev & Guedes Soares (eds)
© 2020 Taylor & Francis Group, London, ISBN 978-0-367-40951-7

Controllability studies on fish-shaped unmanned under water vehicle undergoing manoeuvring motions

A.K. Ranjith, S. Janardhanan, V. Chandran & N.J. Gomez
Department of Mechanical Engineering, SCMS School of Engineering and Technology, Ernakulam, India

G. Ilieva
Department of Ship Building, Technical University of Varna, Bulgaria

J. Sygal
Department of Ocean Engineering, Indian Institute of Technology Madras, India

ABSTRACT: Bio-inspired propulsion systems have many advantages over the conventional ones. They are found to be noiseless and eco-friendly. Most of the aquatic locomotion makes use of oscillations, paddling and water-jet for producing net thrust on the body. In this paper a box-fish shaped unmanned underwater vehicle (UUV) has been considered for studying its controllability. A RANS based CFD method has been implemented for simulating manoeuvring motions in heave and pitch to obtain the forces and moments during such motions.

1 INTRODUCTION

Bio-inspired propulsion is a much researched field these days. The fact that, the noise and vibrations produced during the operation of conventional propellers have adversely affected the bio-diversity of oceans, has made bio-inspired propulsion more enticing to mankind. Getting rid of the conventional rotary components of a propulsion system completely is also not practical. Ocean transport do contribute to a mammoth scale of world's economy. Hence there should be a balance between bio-inspired flapping foil as well as the conventional propulsion systems so that we do not tamper much with the ecological systems and at the same time do contribute to the economy.

Nature is known as the master engineer. The efficiency of propulsion of some aquatic animals have struck us in awe and the values of their efficiency have far outperformed those of man-made vehicles. Now it is time to have a few such vehicles operating in the oceans. There have been many studies in the past decades concentrating on the flapping foil mechanisms on ocean vehicles: both surface and sub-sea. Most of them focused on the determination of propulsive efficiency while others on the controllability.

1.1 *Understanding the locomotion of fish*

The locomotion of the fish is indeed complex yet efficient. Various fins involved in the locomotion or swimming are shown in Figure 1.

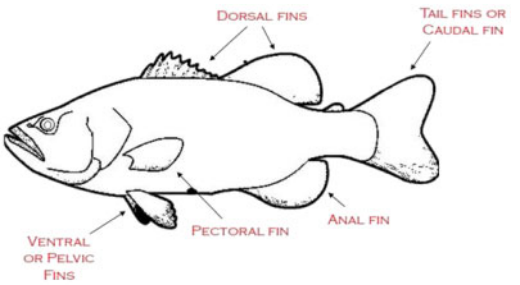

Figure 1. Various fins on the body of a fish.

Fishes swim using all the fins. The locomotion a fish swimming with tail fin or the caudal fin and the trunk is broadly classified into angulliform, subcarangiform, carangiform, thunniform and ostraciiform (Figure 2). From angulliform to ostraciiform the locomotion gets simplified with the deteriorating involvement of the trunk as the undulations of the entire trunk reduces to mere oscillations of the tail during swimming. Locomotion of the fish with varying involvement of the trunk and tail is shown in Figure 3.

In ostraciiform models, the undulation is confined mostly to the caudal fin without moving the body. The thrust for this model is generated with a lift-based method, allowing cruising speeds to be maintained for long periods. This form is considered to be the simplest of all for carrying out mathematical studies. A UUV with hull form geometrically similar to

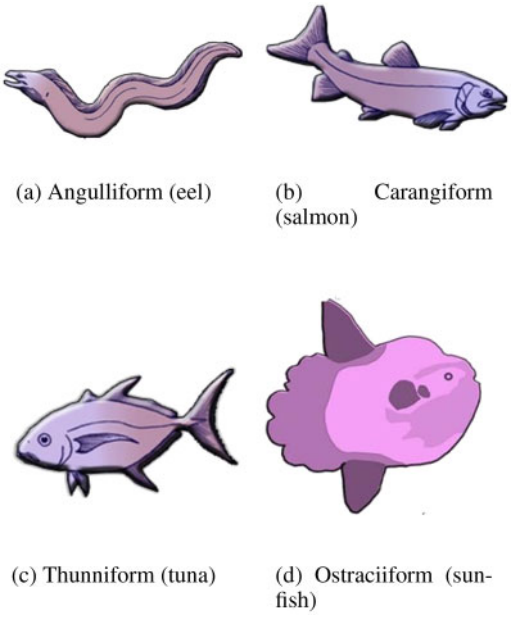

Figure 2. Fish with different types of tail locomotion.

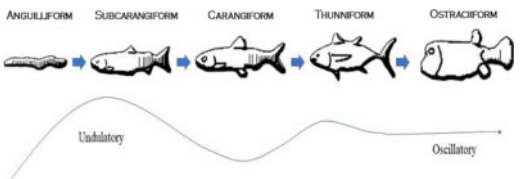

Figure 3. Undulatory motion of the entire trunk to oscillatory motion of the tail.

that of a box-fish, a typical ostraciiform model undergoing manoeuvring motions in heave and pitch, has been analysed for controllability in the present study. UUVs also known as underwater drones are vehicles with no humans onboard during the course of their mission. There are basically two types of UUVs-autonomous underwater vehicle (AUV) and remotely operated vehicle (ROV). AUVs are more or less like robots not entailing human intervention throughout their mission while ROVs are remotely operated from a ground station.

In the case of present work, the vehicle's hull form is more important than its mode of operation. Guidance and control are very important aspects in the design of marine vehicles no matter whether they are surface or underwater vehicles. A motion planning and control system was developed for autonomous surface vehicles by Hinostroza, Guedes Soares, & Xu 2018. This work aims at achieving the first step in controllability predictions-determination of forces and moments during manoeuvring motions. A linear mathematical model combined with a RANS based CFD method has been used for obtaining the thrust generated during the

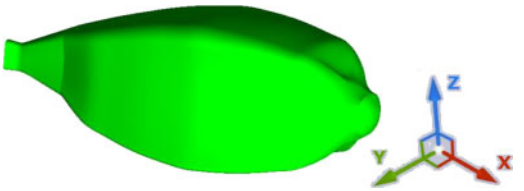

Figure 4. Three dimensional representation of the box-fish shaped UUV.

Table 1. Principal particulars of the UUV.

Dimension	Size (metres)
Length (L)	1.3
Breadth (B)	0.5
Depth (D)	0.5

oscillatory motions of the tail with ANSYS FLUENT as the solver. The forces and moments acting on the hull form in both static and dynamic manoeuvres have been estimated. This paper is an initial step towards the controllability and stability prediction of fish-shaped UUVs which could be used in search and rescue as well as surveillance missions. Hence it is imperative to predict the trajectory of such vessels well in advance through controllability studies of its hull form.

It is quite evident that the ostraciiform type of locomotion is the simplest mode of locomotion. A design based on this type of locomotion will be obviously the most feasible for a UUV. The studies on ostraciiform type of locomotion was reported by Blake 1977. The study made some interesting observations. For slow progression, the caudal fin inclination with the longitudinal axis of the body is about 3 to 6 deg while for fast progression, the angle is 35 deg. 3-D manoeuvring studies were carried out on a fish-like robot by Wu, Yu, Su, & Tan 2014. The robotic fish here was fabricated using multi-link joints to obtain the agility during swimming and hence better manoeuvrability. The present study considers the controllability aspects of a box-fish by numerically simulating the manoeuvring motions.

Not much work has been reported on the determination of hydrodynamic derivatives of the body form for assessing the vessels controllability. This paper presents a method for numerically evaluating the hydrodynamic forces and moments-an initial step towards the estimation of hydrodynamic derivatives and thereby the controllability of a box-fish shaped underwater vehicle.

2 UUV GEOMETRY

A box fish in its three dimensional configuration is shown in Figure 4. The principal particulars of the fish are given in Table 1.

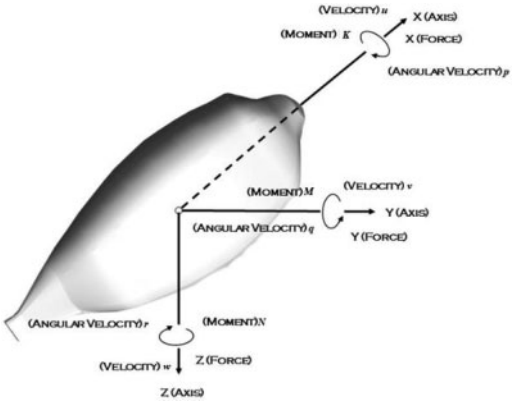

Figure 5. Co-ordinate system used in the study.

3 MATHEMATICAL MODEL

The Cartesian co-ordinate system of the UUV is shown in Figure 5. The conventional North-East-Down (NED) system is followed here.

A linear mathematical model describing the manoeuvring motions of the UUV is represented by Equations (1) through (6)

$$X = X_{\dot{u}}\dot{u} + X_{u|u|}u^2 + X_w w + X_q q + X_\delta \delta + X_T \quad (1)$$

$$Y = Y_{\dot{v}}\dot{v} + Y_v v + Y_p p + Y_r r + Y_\delta \delta \quad (2)$$

$$Z = Z_{\dot{w}}\dot{w} + Z_w w + Z_u u + Z_q q + Z_\delta \delta \quad (3)$$

$$K = K_{\dot{p}}\dot{p} + K_p p + K_v v + K_r r + K_\delta \delta \quad (4)$$

$$M = M_{\dot{q}}\dot{q} + M_q q + M_w w + M_u u + M_\delta \delta \quad (5)$$

$$N = N_{\dot{r}}\dot{r} + N_r r + N_v v + N_p p + N_\delta \delta \quad (6)$$

where subscript T represents thrust and δ, the rudder angle.

4 NUMERICAL EVALUATION OF CONTROLLABILITY IN VERTICAL PLANE

4.1 *Numerical modelling and meshing*

For studying the hydrodynamic forces and moments on the UUV during manoeuvring motion there are two basic methods, viz. numerical and experimental. While experimental methods involve prohibitively expensive and rare facilities, numerical methods offer the ease of bringing tedious tasks to desks. However numerical methods have not yet become self sufficient to completely replace experiments. They definitely offer promising inputs to the conceptual design. In this paper an attempt has been made to simulate the manoeuvring motions in the vertical plane of the UUV's motions.

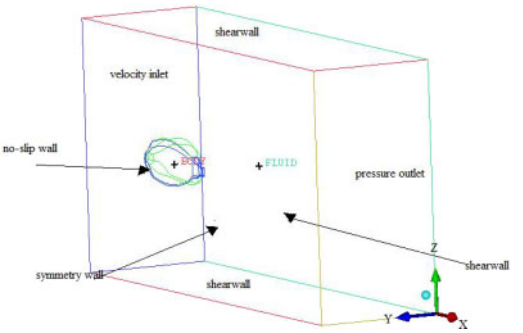

Figure 6. Computational domain with its boundaries.

Geometric modelling and meshing has been carried out using the commercial package ANSYS ICEM CFD. Figure 6 shows the computational domain. Its extends are $2.0L \leq x \leq 5.0L$, $2.0L \leq y \leq 2.0L$ and $0 \leq z \leq 2.0L$.

An unstructured meshing strategy is employed here. The minimum cell size has been calculated following the method described by Chandran, Janardhanan, Menon, et al. 2018.

Boundary layer thickness and the near wall element size have been calculated from boundary layer theory. The thickness of laminar sub-layer is obtained from Equation (7) (Schlichting & Gersten 2016).

$$\delta' = \frac{11.6v}{V^*} \quad (7)$$

where V^* is the frictional velocity given by Equation (8)

$$V^* = \sqrt{\frac{\tau_0}{\rho}} \quad (8)$$

and τ_0, the wall shear stress, is obtained as in Equation (9).

$$\tau_0 = \frac{0.664}{\sqrt{Re_L}} \cdot \frac{\rho V^2}{2} \quad (9)$$

where, V is the flow velocity and Re_L the length based Reynolds number.

The mesh generated in the computational domain in shown in Figure 7(a). The magnified view around the fish body is shown in figure 7(b).

A velocity corresponding to $Re = 0.5 \times 10^6$ is imposed on the velocity inlet. The outlet is considered to be a pressure outlet. Half-fish model is used with the plane holding mid x-y plane as a symmetry wall. Non-slip boundary condition is assigned to the UUV body and slip walls to the far-field.

4.2 *Steady-state predictions*

Steady simulations are carried out with $k - \omega$ SST two equation model. PISO scheme is used for pressure velocity coupling. The convergence criteria is set

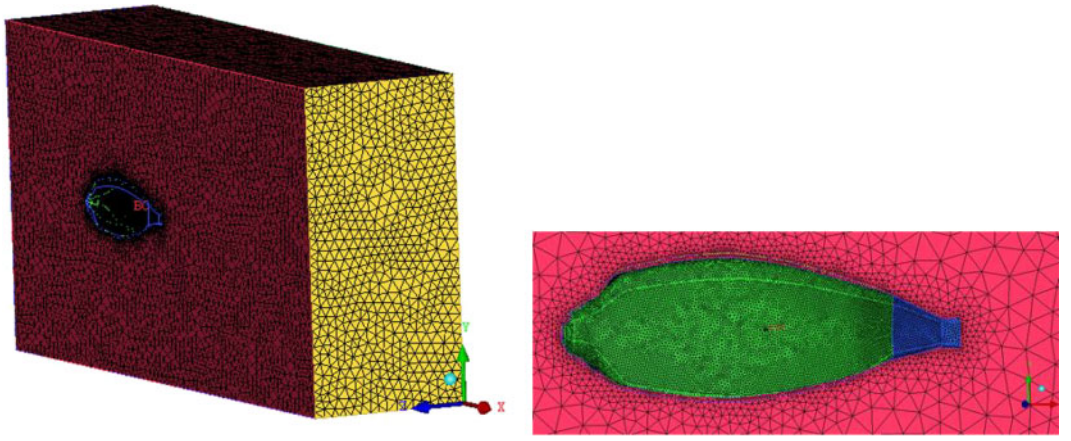

(a) Mesh in the domain

(b) Magnified view around the UUV body

Figure 7. Unstructured mesh for computation.

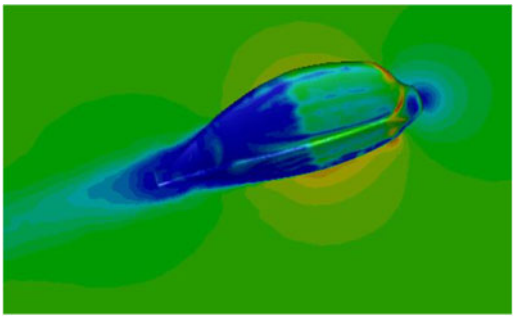

Figure 8. Dynamic pressure contours on the half-UUV.

to 10^{-7}. The simulations have been carried out using ANSYS FLUENT version 18.1. Dynamic pressure contours on the half-fish model is shown in Figure 8.

4.3 *Static manoeuvre simulations*

As the 3D simulations were time consuming, for faster predictions, a cut section of the UUV in the 2D plane is used for further analysis. The coefficients of drag (C_D) and lift (C_L) obtained from 3D simulations discussed in the previous section have been used as the reference. The challenge in 2D CFD simulations to yield results close to 3D simulations lies in defining the reference value in the third dimension. As this value remains constant and doesn't consider the variation in the geometry of the model, 2D computations provide only approximate values. Nevertheless, these computations provide enough insights into the flow physics as well as hydrodynamic forces and moments in the initial phase of any design.

Simulations have been carried out by varying the drift angle (β) from 0 to 12.5 deg in the vertical plane. The velocity contours around the UUV obtained from the simulation are presented in Figure 9. Figures from 9 (a) to 9 (f) represents different contours for various drift angles.

4.4 *Propulsion tests*

Propulsion tests have been carried out on a 2D model through prescribed rigid body motions on the tail using the displacement function given by Equation 10

$$\phi = -\phi_a \sin(\omega t) \tag{10}$$

through the user defined functions (UDF) module of the solver.

Here ϕ is the sinusoidal tail oscillation about y-axis, ϕ_a the amplitude of motion taken here as 12.5 deg, ω is the angular frequency, 0.5 rad/s and t, the instantaneous time. The wake oscillations indicating the effective production of thrust is depicted in Figure 10.

4.5 *Dynamic manoeuvre simulations*

Hydrodynamic forces and moments are predicted here by simulating the manoeuvring motions in heave and pitch. Roll motions are not considered.

The sinusoidal motions in heave and pitch have been brought in using UDF module of the solver. The displacement functions in pitch and heave are as given by Equations 10 and 11 respectively.

$$z = z_a \sin(\omega t) \tag{11}$$

Here z_a is taken as $D/4$. Simulations have also been carried out imposing combined heave and pitch on the UUV body. Contours of total pressure around the UUV body in heave, pitch and combined motions are shown in Figures 11, 12 and 13 respectively.

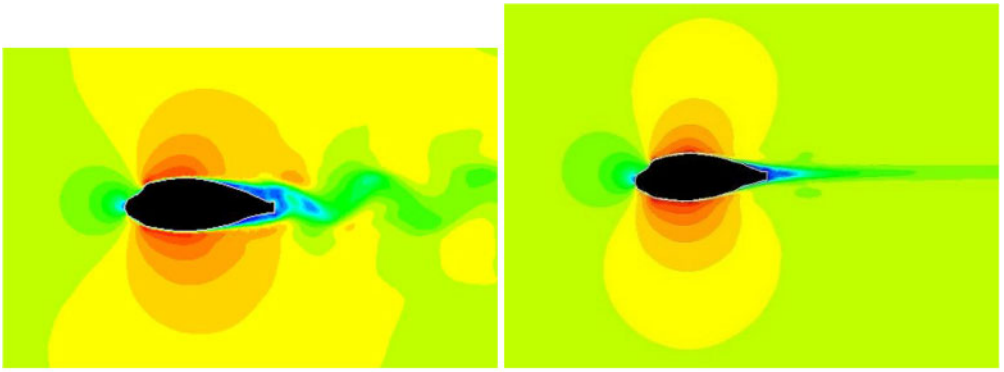

(a) 0 deg

(b) 2.5 deg

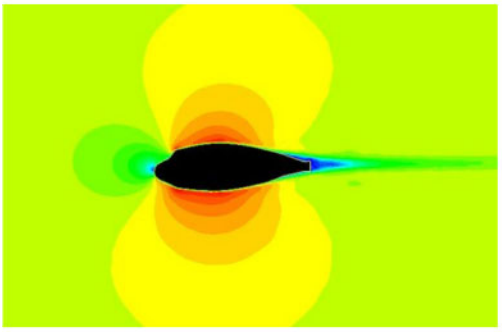

(c) 5 deg

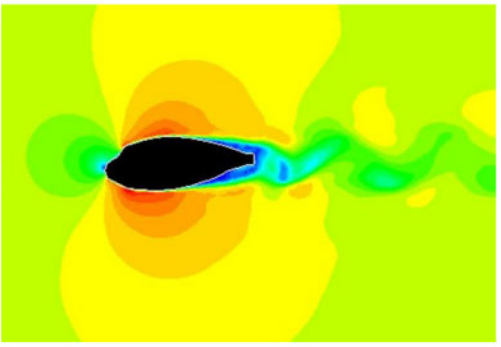

(d) 7.5 deg

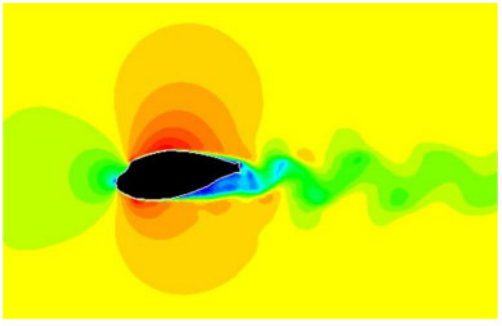

(e) 10 deg

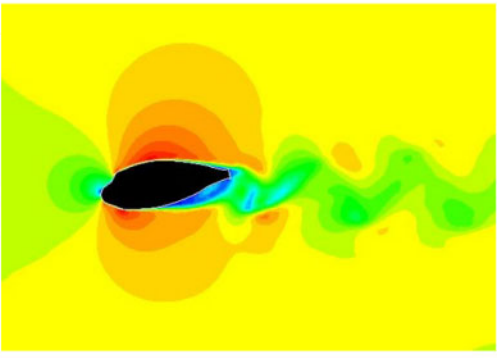

(f) 12.5 deg

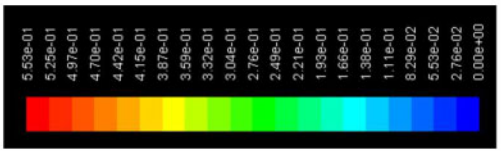

(g) Velocity Range

Figure 9. Velocity contours around the UUV at various angles of attack.

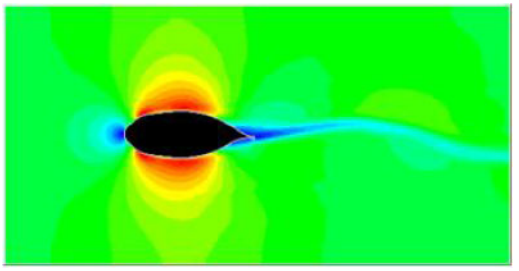

Figure 10. Wake oscillations due to tail motions.

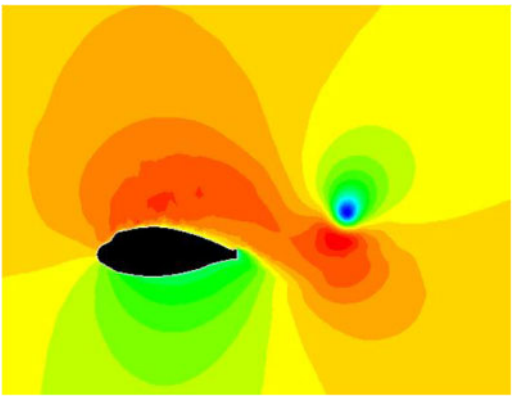

Figure 11. Total pressure contours in heave.

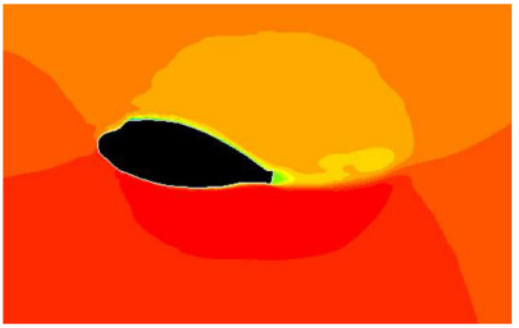

Figure 12. Total pressure contours in pitch.

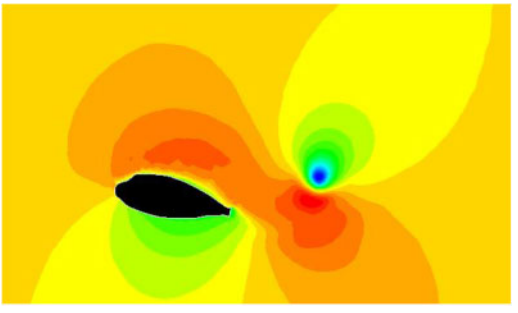

Figure 13. Total pressure contours in combined mode.

5 RESULTS AND DISCUSSIONS

In the present work manoeuvre motion simulations have been carried out on an ostraciiform locomotion inspired box-fish shaped UUV. At the outset, steady state simulations were carried out on a half model of the UUV for $Re = 0.5 \times 10^6$. The simulation yielded the value of drag coefficient, C_D as 0.019 and lift coefficient, C_L as 0.0684. The 2D simulations with an approximation of the third side yielded $C_D = 0.021$ and $C_L = 0.074$. The results show that 2D simulations can yield better results. Net surge and heave forces have been estimated using the Equations (12) and (13) respectively. As there are not much literature on this study, the results could not be verified.

$$X = F_D \cos\beta + F_L \sin\beta \quad (12)$$

$$Z = -F_D \sin\beta + F_L \cos\beta \quad (13)$$

Variation of the surge force, heave force and pitch moments with the angle of attack, β are shown in Figures 14, 15 and 16 respectively. The plots are also supplemented by a smoothing trend line.

The prediction of hydrodynamic forces and moments in the case of box-fish like bodies is not as straight forward as in the case of streamlined ships and submarines. The body being bluff, sheds vortices at moderate angles (say 7.5 deg) of attack which shows a sudden drop in surge and heave forces as well as in pitch moment. Later beyond 10 deg, the formation of vortices stabilizes and are expected to contribute

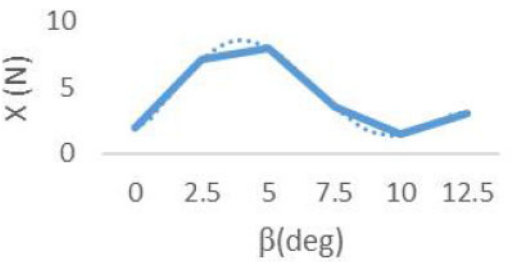

Figure 14. Variation of surge force with angle of attack.

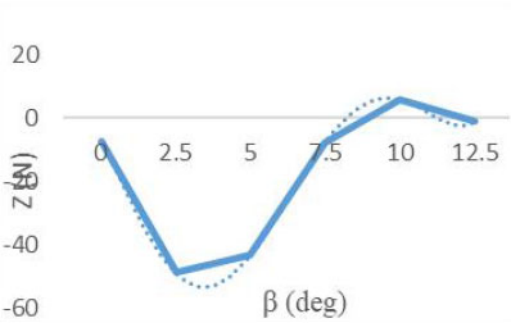

Figure 15. Variation of heave force with angle of attack.

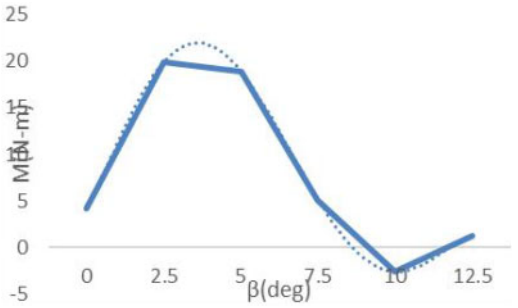

Figure 16. Variation of pitch moment with angle of attack.

to induced components of surge, heave and pitch and hence a rise in the trend is seen. The static manoeuvre simulation tests on further analysis provide the w dependent derivatives.

The propulsion simulation using the oscillation of the tail show an oscillating wake with very weak vortices shedding and disappearing in no time. Hence ostraciiform fish exhibits sluggish locomotion. The maximum thrust generated due to tail motion is found to be $X_T = 2.4N$.

Time histories of surge force, heave force and pitch moment when the UUV is subjected to pure sinusoidal heave motion is shown in Figure 17 plotted for one complete time period of oscillation ($12.56\,rad/s$).

Similarly, the time histories of forces and moment in pitch and combined mode is shown in Figures 18 and 19.

These plots reveal that box-fish, due to its asymmetry about y-z plane doesn't produce symmetrical surge forces while its symmetry in x-z as well as x-y planes resulted in symmetrical heave forces and pitch moments. From heave simulations, the hydrodynamic coefficients that can be evaluated are X_w, Z_w and M_w. From the pitch simulations the derivatives X_q, Z_q and M_q can be evaluated. Combined mode simulations yield coupled derivatives which are not of interest to this paper. The other derivatives can also be evaluated considering the motions in the horizontal plane and also by considering roll into account.

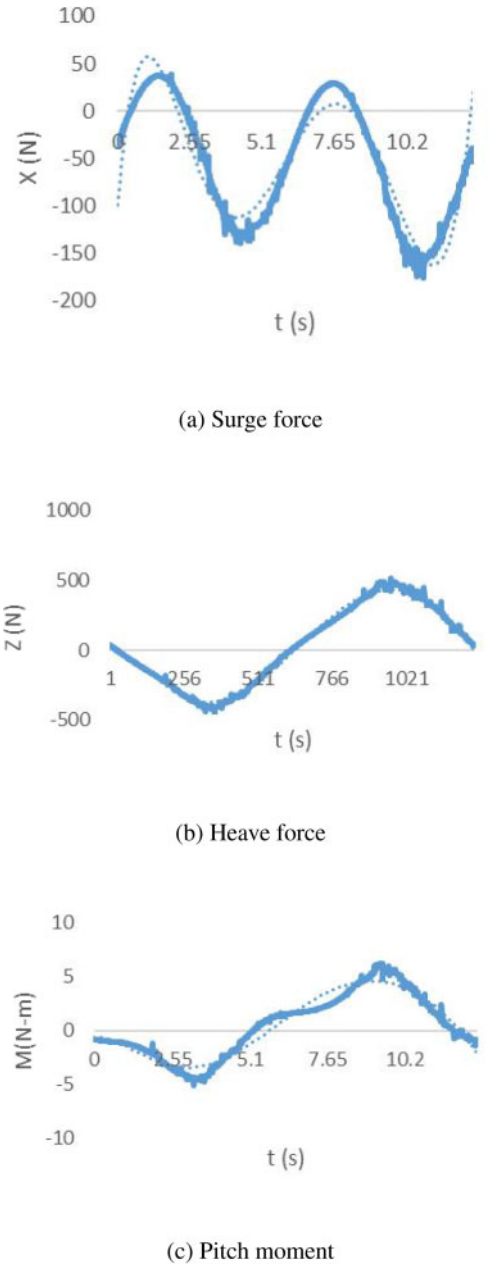

Figure 17. Time histories of forces and moment in heaving motion.

6 CONCLUSIONS

Box-fish owing to its non-streamlined shape has poor controllability. They need extra thrust from the pectoral fins to supplement the thrust produced by the caudal fin. Their tail length is too short to generate reverse Von-Kármán vortex street of vortices for improved power. This tail form helps the fish in sustaining power for a longer time. Nevertheless, this work provides an initial frame work for the estimation of hydrodynamic derivatives for a UUV in the form of a box fish-the simplest possible mode of implementation for bio-inspired propulsion. 2D results have helped us in reasonable qualitative predictions. Quantitatively, the results are yet to be verified either with experimental or published ones. For more accurate prediction, overset grids and 3D models are suggested.

7 FUTURE WORK

Nature has its own way of compensating for the shortcomings imposed on its own creation. The carapace on the fish's body is believed to reduce drag and direct

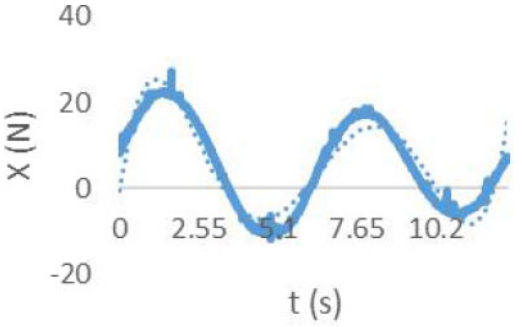

(a) Surge force

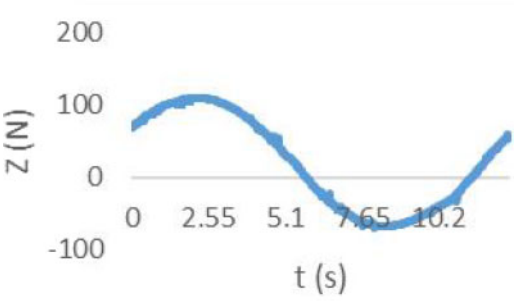

(b) Heave force

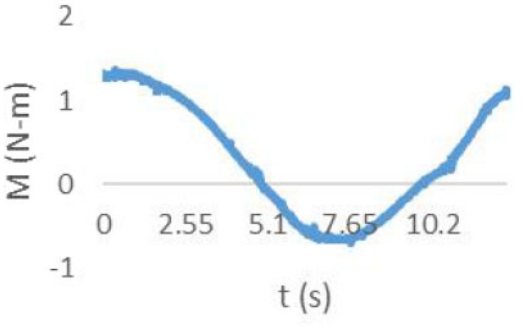

(c) Pitch moment

Figure 18. Time histories of forces and moment in pitching motion.

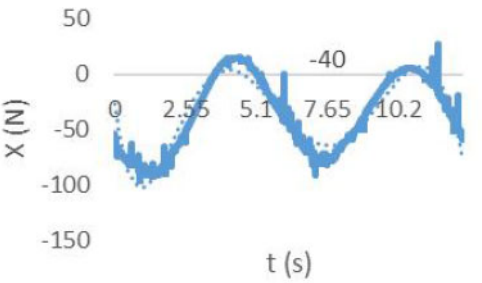

(a) Surge force

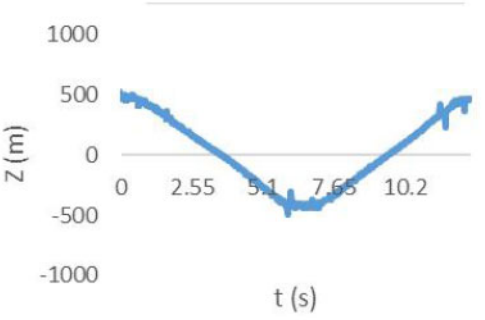

(b) Heave force

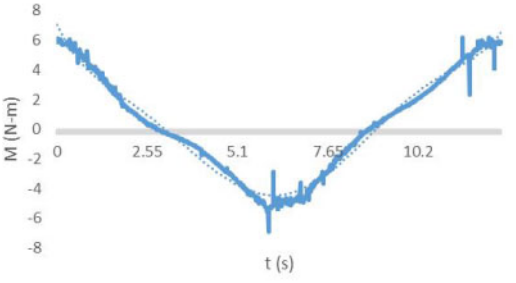

(c) Pitch moment

Figure 19. Time histories of forces and moment in surge motion.

flow such that the fish attains better manoeuvrability (Van Wassenbergh, van Manen, Marcroft, Alfaro, & Stamhuis 2015). Moreover, the role of the pectoral fins in augmenting the thrust produced by caudal fin is unexplored in the present work. The present work will be extended with the inclusion of carapace and pectoral fins in the future works. The hydrodynamic forces and moments will be analyzed using a Fourier series method (Janardhanan & Krishnankutty 2009) for obtaining the hydrodynamic derivatives of the hull form.The trajectories of the UUV in standard manoeuvres such a turning circle and zig-zag will be predicted to finally arrive at its controllability, counter-controllability and stability characteristics.

REFERENCES

Blake, R. (1977). On ostraciiform locomotion. *Journal of the Marine Biological Association of the United Kingdom 57*(4), 1047–1055.

Chandran, V., S. Janardhanan, V. Menon, et al. (2018). Numerical study on the influence of mass and stiffness ratios on the vortex induced motion of an elastically mounted cylinder for harnessing power. *Energies 11*(10), 2580.

Hinostroza, M., C. Guedes Soares, & H. Xu (2018). Motion planning, guidance and control system for autonomous surface vessel. In *ASME 2018 37th International Conference on Ocean, Offshore and Arctic Engineering*, pp. V11BT12A016–V11BT12A016. American Society of Mechanical Engineers.

Janardhanan, S. & P. Krishnankutty (2009). Prediction of ship maneuvering hydrodynamic coefficients using numerical towing tank model tests. In *12th Numerical Towing Tank Symposium*.

Schlichting, H. & K. Gersten (2016). *Boundary-layer theory*. Springer.

Van Wassenbergh, S., K. van Manen, T. A. Marcroft, M. E. Alfaro, & E. J. Stamhuis (2015). Boxfish swimming paradox resolved: forces by the flow of water around the body promote manoeuvrability. *Journal of the Royal Society Interface 12*(103), 20141146.

Wu, Z., J. Yu, Z. Su, & M. Tan (2014). Implementing 3-d high maneuvers with a novel biomimetic robotic fish. *IFAC Proceedings Volumes 47*(3), 4861–4866.